HEAT TRANSFER AND PRESSURE DROP MEASUREMENT FOR SQUARE CHANNELS WITH V-SHAPE RIBS AT HIGH REYNOLDS NUMBERS

A Thesis

by

NAWAF YAHYA ALKHAMIS

Submitted to the Office of Graduate Studies of
Texas A&M University
in partial fulfillment of the requirements for the degree of

MASTER OF SCIENCE

August 2009

Major Subject: Mechanical Engineering

HEAT TRANSFER AND PRESSURE DROP MEASUREMENT FOR SQUARE CHANNELS WITH V-SHAPE RIBS AT HIGH REYNOLDS NUMBERS

A Thesis

by

NAWAF YAHYA ALKHAMIS

Submitted to the Office of Graduate Studies of
Texas A&M University
in partial fulfillment of the requirements for the degree of

MASTER OF SCIENCE

Approved by:

Chair of Committee,	Je C Han
Committee Members,	Mahmoud El-Halwagi
	Sai Lau
Head of Department,	Dennis O'Neal

August 2009

Major Subject: Mechanical Engineering

ABSTRACT

Heat Transfer and Pressure Drop Measurement for Square Channels with V-shape Ribs at High Reynolds Numbers. (August 2009)

Nawaf Yahya Alkhamis, B.Sc King Abdulaziz University

Chair of Advisory: Dr. Je C Han

In previous studies, the thermal performance of ribbed channels was studied for Reynolds numbers up to 100,000 with different rib shapes. In more recent studies, the thermal performance of ribbed channels was studied up to Reynolds numbers of 400,000 for angled ribs to cover the range of internal cooling inside land-based gas turbines. Previous studies also show that the thermal performance of V-shaped ribs is better than the angled ribs. In this study, the Reynolds number from 30,000 to 400,000 is studied with V-shaped ribs. The blockage ratio e/D is 0.1, 0.15, and 0.18 and spacing ratio P/e is 5, 7.5, and 10. The results show that the Nusselt number enhancement decreases when the Reynolds number increases. The friction factor is found to be independent of The Reynolds number. The thermal performance decreases when the Reynolds number increases. Correlations for the Nusselt number and the friction factor as function of Re, e/D, and P/e are developed.

ACKNOWLEDGEMENTS

I am grateful to Dr. J. C. Han for giving me the opportunity to do research in the area of experimental heat transfer. I am appreciative that Dr. Mahmoud El-Halwagi and Dr. Sai Lau have served on my committee and gave me suggestions on my research and thesis. I also thank the experienced partners in the lab who always gave me helpful advice and solutions. I also thank King Abdulaziz University for giving me a scholarship to study at Texas A&M University.

NOMENCLATURE

C_p	Specific Heat
D	Hydraulic Diameter
e	Rib Height
f	Fanning Friction Factor
F	Thermal Performance
f_0	Friction Factor Corresponding to Smooth Channel Flow
H	Height of Channel
k	Thermal Conductivity
Nu	Nusselt Number
Nu0	Nusselt Number Corresponding to Smooth Channel Flow (Ditus-Boelter)
P	Spacing Between Consecutive Ribs
Pr	Prandtl Number
Re	Reynolds Number
AR	Aspect Ratio
μ	Dynamic Viscosity
ρ	Density

TABLE OF CONTENTS

Page

ABSTRACT iii

ACKNOWLEDGEMENTS iv

NOMENCLATURE v

TABLE OF CONTENTS vi

LIST OF FIGURES vii

1. INTRODUCTION 1

2. TEST SECTION 5

3. DATA REDUCTION 8

4. RESULTS AND DISCUSSION 11

    4.1 Heat transfer 11
    4.2 Friction losses 16
    4.3 Thermal performance 18

5. ERROR ANALYSIS 20

    5.1 Heat transfer uncertainty 20
    5.2 Friction factor uncertainty 21

6. CONCLUSIONS 23

REFERENCES 24

VITA 26

LIST OF FIGURES

Page

Figure 1 Schematic of flow loop... 5

Figure 2 Various geometries tested... 7

Figure 3 Normalized Nusselt number ratios for a smooth channel 11

Figure 4 Local normalized Nusselt number ratio 12

Figure 5 Schematic of flow over V-shape ribs indicating the effect of rib spacing for rib height... 13

Figure 6 Average normalized Nusselt number with Reynolds number.......................... 14

Figure 7 Fully developed ribbed side average Nusselt number obtained in various test cases.. 15

Figure 8 Friction factors for various geometry... 17

Figure 9 Ribbed side average Nusselt number enhancement ratio plotted against friction factor penalty ratio.. 18

Figure 10 Thermal performance plotted with Reynolds number..................................... 19

1. INTRODUCTION

Gas turbines are used in land-based power plant to produce electricity and in aircrafts or ships. According to the thermodynamics concept, gas turbine performance is improved when the gas temperature, which exit from combustion chamber, increases. This high gas temperature can melt turbine blades and cause thermal stress. Cooling turbine blades is necessary to prevent failure. There are two technologies to protect turbine blades from melting and thermal stresses; film cooling to protect the blades surface from hot stream, and internal cooling passage to absorb heat from blades. Film cooling involves injects relatively cool air on the surface of the blade to protect the hole and downstream[1]. On the internal cooling side, impingement jets are used in leading edge. The leading edge receives more heat from the main stream, so the impingement jets are used to cool the leading edge portion. The space in the trailing edge is small, so pin fins are used to cool the trailing edge portion. Ribbed channels are used to cool the middle portion because the impingement jets and pin fins produce high friction losses. In the ribbed channels there are many parameters which effect on the heat transfer and pressure losses such as the Reynolds Number, aspect ratio, ribs height, ribs space, and rib shape.

This thesis follows the style of Journal of Turbomachinery.

Han et al. [2] studied heat transfer and pressure losses with different angle ribs in square channels and rectangular channels with aspect ratio of 2 and 4. The rib angles for both square and rectangular channels were 90°, 60°, 45°, and 30°. The Re was from 10000 to 60000. The higher thermal performance in the square channel was 30° rib angle and the higher thermal performance in the rectangular channel was 45° rib angle. The higher heat transfer with higher pressure drop in the square channel was 60° rib angle. The higher heat transfer with the higher pressure drop in the rectangular channel was 90° rib angle. Han et al. [3] studied heat transfer and pressure losses with different rib shapes in a square channel. the rib shape was Parallel angle ribs, Crossed angle ribs and V-shape ribs. The angles for the parallel and crossed were 45°, 60°, and 90°. The angles for the V-shape ribs were 45° and 60°. The Re was from 15000 to 90000. The 60° and 45° V-shape have higher thermal performance then 60° and 45° angle rib. Han et al. [4] studied heat transfer and pressure losses with continuous angled ribs and broken angle ribs with angles of 90°, 60°, and 45°, continuous V-shape and broken V-shape ribs with angles of 60° and 45° in square channel. The Re was from 15000 to 90000. The broken V-shape with of 60° angle has the best thermal performance among other geometry. Lau et al. [5] studied heat transfer and friction losses with V-shape ribs with angles of 45°, 60°, 90°, 120°, and 135° in the square channel. The Re was from 10000 to 60000. The V-shape with 60° angle has the highest thermal performance in this study. Park et al. [6] studied heat transfer and pressure losses with different angle ribs in square channel and rectangular channels with aspect ratio 1/4, 1/2 ,1, 2 and 4. The rib angles for both square and rectangular channels were 90°, 60°, 45°, and 30°. The Re was from 10000 to 60000. The low aspect ratio has the highest thermal performance. For low aspect ratio, the 45°

and 60° have the highest thermal performance. For square channel, the 60° and 45° have the highest thermal performance. For large aspect ratio, 30° and 45° have the highest thermal performance. Taslim et al. [7] studied Heat transfer and friction losses with angled 90° and 45° ribs and V-shape ribs. The Re was from 10000 to 60000. Ekkad et al. [8] studied heat transfer and pressure losses with different angle ribs, 60° continuous V-shape and broken V-shape ribs in two passage square channel. The Re was from 6000 to 60000.

There are many studies of the effect of the ribs height and rib spacing. Taslim et al. [9] study the effect of P/e and e/D effect on the heat transfer and friction losses with 90° sharp angle ribs, and 90° around angle ribs in rectangular channel with aspect ratio .5 and .55(Aspect ratio= smooth: ribbed). For aspect ratio equal .5, e/D was from .15 to .285 and P/e was from 5 to 14. For aspect ratio equal .55, e/D was from .17 to .275 and P/e was 5. Every e/D and aspect ratio has optimum P/e. Lau et al. [5] studied the effect of P/e on the heat transfer and friction losses for 90° angled ribs and V-shape 60°, and 120° angled ribs in square channel. P/e was 10 and 20. The 60° V-shape ribs with P/e equal 10 has highest thermal performance. Taslim et al. [7] study the effect of e/D effect on the heat transfer and friction losses with 90° angled ribs, 45° angled ribs, and V-shape ribs. The Re was from 5000 to 30000. The e/D was 0.085, 0.125 and 0.167. P/E was 10. In the low e/D, the V-shape ribs have the highest thermal performance. With e/D equal .125 and .165, the 45° angled ribs have the highest thermal performance. Taslim et al. [10] study the effect of P/e and e/D on the heat transfer and friction losses 90° sharp angle ribs, and 90° around angle ribs in square. The e/D was .133, .167 and .25 and P/e was 5, 7, 8.5, and 10. P/e=8.5 and 10 have the highest thermal performance. The thermal performance increase when the e/D increases. Taslim et al. [11] studied the effect of e/D effect on the heat transfer and friction losses with 90° angled ribs, 45° angled ribs, V-shape ribs, and discrete angled ribs. The Re was from 5000 to 30000. The e/D was .085, .125 and .167. P/e was 10. In the low e/D, the V-shape ribs have highest thermal performance. With e/D equal .125 and .165, the 45° angled ribs has highest thermal performance. Taslim et al. [12] studied the effect of P/e and e/D on the heat transfer and friction losses 90° sharp angle with low aspect ratio (aspect ratio of ribs= .667) ribs in the square channel. The e/D was .133, .167, and .25 and P/e was 5, 8.5, and 10. P/e= 10 has the highest thermal performance. The thermal performance increases when the e/D increases.

The Reynolds number also effects the thermal performance. Rallabandi et al. [13] studied the effect of P/e and e/D on the heat transfer and friction losses with 45° sharp angle ribs in square channel at high Reynolds number. The Re was from 30000 to 400000. e/D was 0.1, 0.15, and 0.18 and P/e was 5, 7.5, and 10. Rallabandi et al. [14] studied the effect of P/e and e/D on the heat transfer and friction losses with 45° round angle ribs in square channel at high Reynolds number. The Re was from 30000 to 400000. e/D was 0.1, 0.15, and 0.18 and P/e was 5, 7.5, and 10.

In this study, the Reynolds number from 30000 to 400000 was studied with V-shape ribs. The blockage ratio was from 0.1, 0.15, and 0.18 and spacing ratio was 5, 7.5, and 10. The correlation was modified for Reynolds number from 30000 to 400000, blockage ratio from 0.1 to 0.18, and spacing ratio from 5 to 10.

2. TEST SECTION

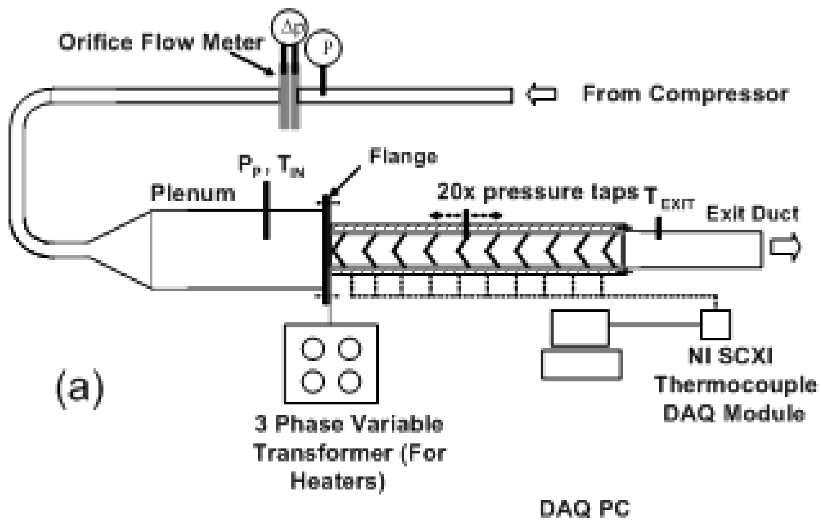

Figure 1 Schematic of flow loop

The air was pressurized to 820 kpa by 3 Ingersoll Rand Oil Free compressors. The capacity of each compressor is 19.7085 m^3/min. There is a ball valve to protect the test section facility. Then the air passes the gas regulator to adjust the air flow. The orifice meter with a 50.8 cm diameter was used to measure the flow rate. The upstream pressure of orifice meter was measured by digital Manometer and differential pressure between upstream and across orifice pressure by inclined manometer. After that, the air enters a plenum then enters to test section with sudden contraction. This contraction helps to generate the aerodynamics and thermal developing regions (see fig. 1). The test section was square channel with 10.16 cm X 10.16 cm. The channel length is 152.4 cm.

The channel was divided into 10 sequential stream-wise regions. Every sequential stream-wise region was built from four copper plates. Every plate was separated by a rubber gasket to minimize the conduction effect between plates. The ribs are made from copper. The ribs are attached on back and front walls by using copper double sided tape. The top and bottom walls remain smooth.

In the Heat transfer experiment, four silicone heaters are attached the channel wall by using spray adhesive. The power in each heater can be controlled separately. Four thermocouples (T-type) attached in the top and back plates and one thermocouple attached in the front and bottom plates. The thermocouples are connected to National Instruments SCXI 1000 Chassis via the NI SCXI 1303 terminal block. The temperatures are measured using the NI Labview Program. The inlet temperature and exit temperature are measured by digital thermometer. The test section was covered by a 4 cm thick Plexiglas housing and thick layer of fiber glass.

In the pressure losses experiment, the top plates have two holes located in 25% and 75% of length to measure the static pressure in each hole by using an inclined manometer or digital manometer. Different rib configurations are summarized in fig 2 and in table 1.

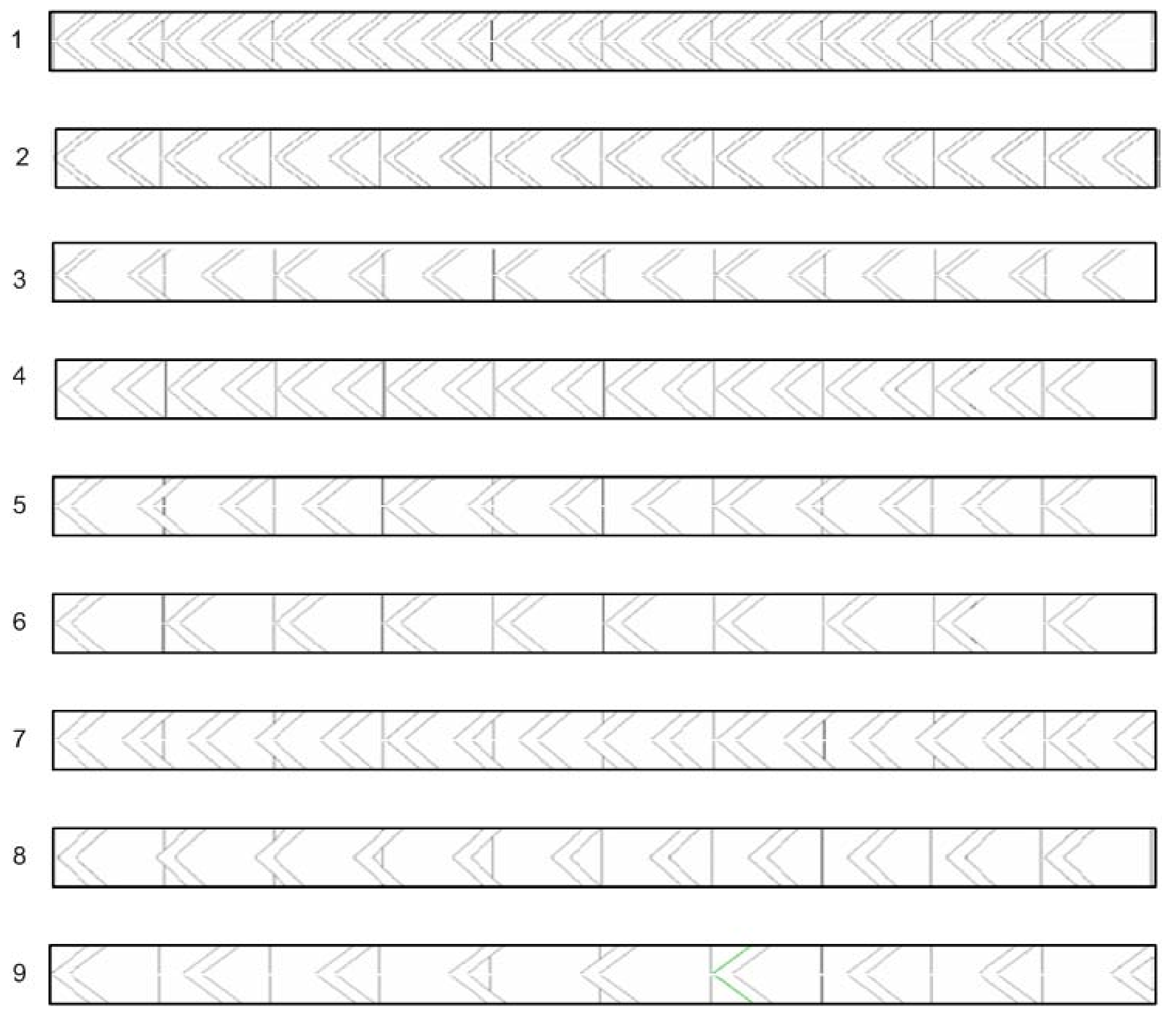

Figure 2 Various geometries tested. detailed parameters corresponding to each test in table 1

Table 1 Geometric details various tests. both heat transfer and friction tests run for all nine cases; each case repeated once

	P/e=5	P/e=7.5	P/e=10
e/D=.1	1	2	3
e/D=.15	4	5	6
e/D=.18	7	8	9

3. DATA REDUCTION

The Reynolds Number was calculated by equation (1)

$$\mathrm{Re} = \frac{UD}{\nu} \tag{1}$$

Where U is the velocity in test section which was calculated by equation (2)

$$U = \frac{m}{\rho H^2} \tag{2}$$

The total heat transfer rate for each wall was calculated by equation (3)

$$Q_{total} = \frac{V^2}{R} \tag{3}$$

The local heat transfer rate for each plate was calculated by equation (4)

$$q = \frac{Q_{total}}{10} - Q_{losses} \tag{4}$$

In the back plates and top plates, the average temperature was calculated to obtain the back plate temperature (T_b) and the top plate temperature (T_t). The bottom plate temperature (T_{bo}) and the front plate temperature (T_f) are measured. The air temperature was calculated by using energy balance in equation (5).

$$\mathrm{T_{air,i}} = \mathrm{T_{air,i-1}} + \frac{\sum \mathrm{q}}{\rho \mathrm{C_p}} \tag{5}$$

Σq is the heat rate from the whole plates inside the sequential stream-wise region. The heat transfer for each plate inside the sequential stream-wise region was calculated by equation (6).

$$h = \frac{q}{A_p (T_w - T_{Air})} \tag{6}$$

The heat transfer coefficient in this study is based on the projected area. The local heat transfer coefficient was calculated in the back plate, front plate, bottom plate and top plate.

The local Nusselt Number is calculated by using equation (7) for back plate, front palate, bottom plate and top plate.

$$Nu = \frac{hD}{k} \tag{7}$$

The average Nusselt number calculated x/D from 15.24 cm to 137.16 cm.

The friction factor was calculated by equation (8)

$$f = \frac{D}{2\rho U^2}\left|\frac{dp}{dX}\right| \tag{8}$$

The dp/dX is slop of least-squares-best-fit line graph in the region in whole test section.

The heat transfer and friction factor in smooth channel calculated by equation (9) and (10)

$$Nu_o = .0323\,\mathrm{Re}^{.8}\,\mathrm{Pr}^{.4} \tag{9}$$

$$f = \frac{.33}{\left(\ln\left(\frac{5.74}{\mathrm{Re}^{.9}}\right)\right)^2} \tag{10}$$

The thermal performance of the ribbed channel define as

$$TP = \frac{\left(\frac{Nu}{Nu_0}\right)}{\left(\frac{f}{f_0}\right)^{\frac{1}{3}}} \tag{11}$$

4. RESULTS AND DISCUSSION

4.1 Heat transfer

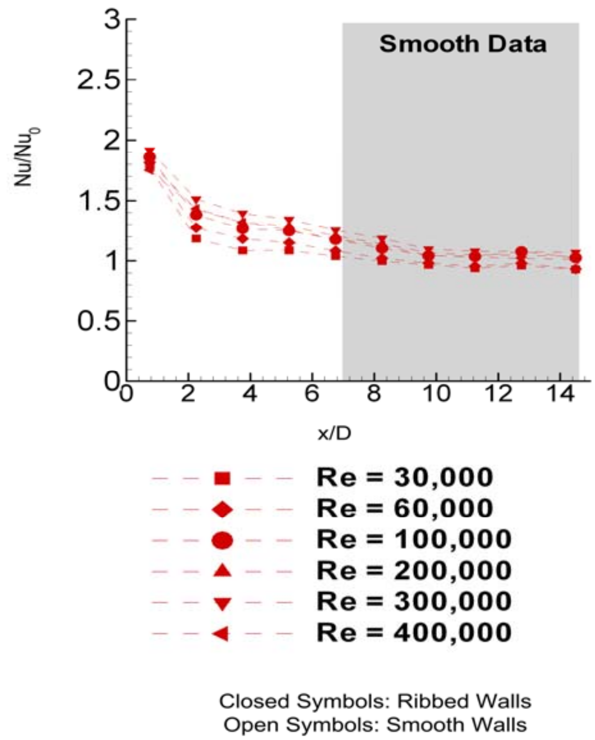

Figure 3 Normalized Nusselt number ratios for a smooth channel

Fig (3) shows the experimental Nusselt number in the smooth channel divided with Ditus-Boelter correlation (Nu/Nu_0). In the low x/D, the value of Nu/Nu_0 significantly is more than 1 and decreases with the x/D decreases due to the boundary developing region. In the large x/D, the value of Nu/Nu_0 becomes 1 due to boundary developed region. The Nusselt numbers in the fully developed region are averaged and plotted against Reynolds Number in fig (7).

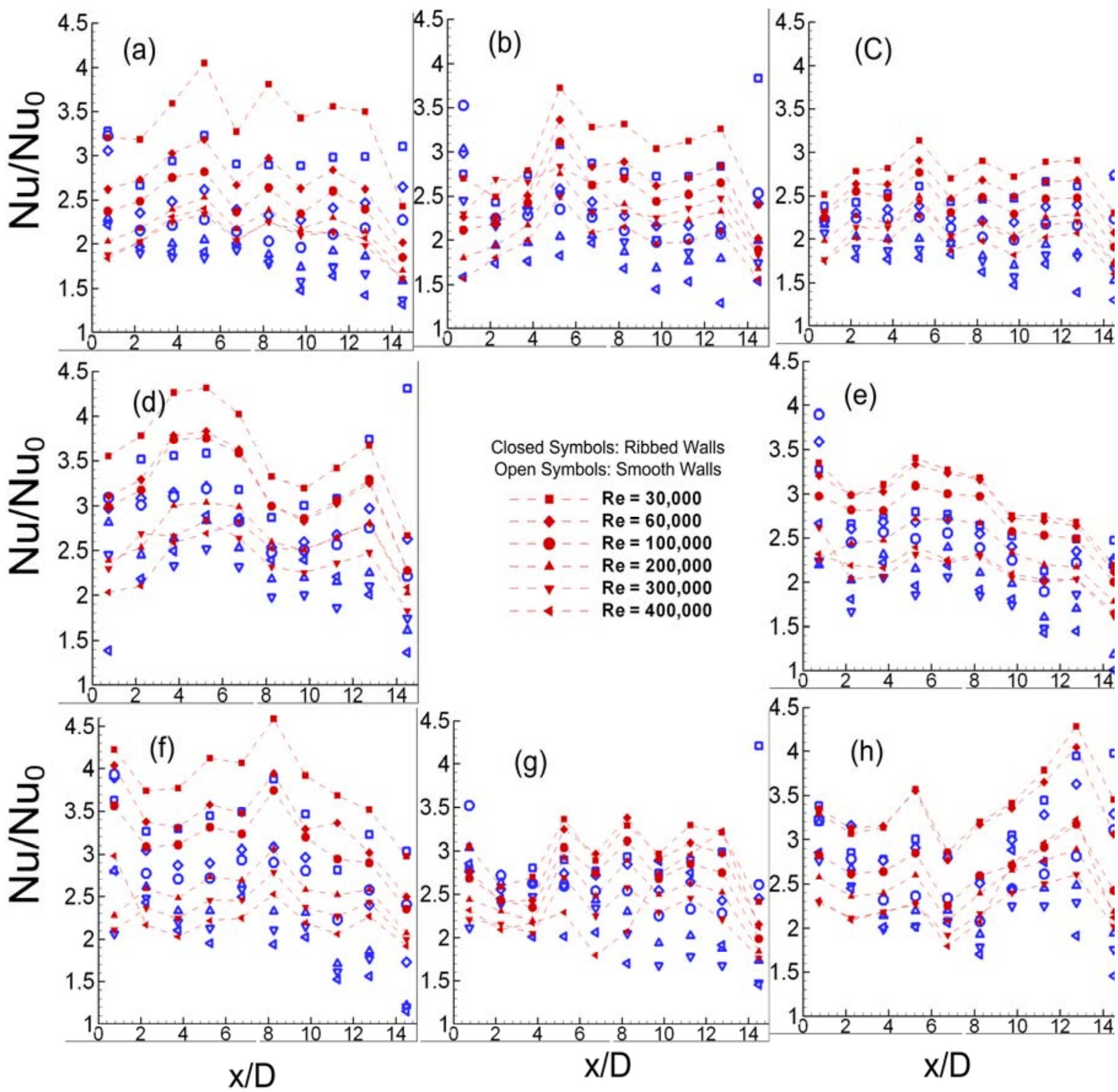

Figure 4 Local normalized Nusselt number ratio for: (a) P/e=5 e/D=.1, (b) P/e=7.5 e/D=.1. (c) P/e=10 e/D=.1, (d) P/e=5 e/D=.15, (e) P/e=10 e/D=.15, (f) P/e=5 e/D=.18, (g) P/e=7.5 e/D=.1, (h) P/e=5 e/D=.1

Fig (4) shows the Normalized Nusselt Number (Nu/Nu_0) with x/D for various rib geometries. The Normalized Nusselt Number (Nu/Nu_0) enhancement increases for both the ribbed side and the smooth side. In the smooth side, the Normalized Nusselt Number (Nu/Nu_0) enhancement increases because the secondary flow impinges on the smooth side. In the ribbed side, the Normalized Nusselt Number (Nu/Nu_0) enhancement increases because the total area increases due to the ribs area and turbulence due to the secondary flow created by ribs. The spacing ratio (P/e) effects the heat transfer enhancement. If the spacing ratio (P/e) decreases the heat transfer enhancement increases because the total area to projected area ratio increases due decreasing spacing ratio and the large number of ribs induce greater secondary flow (see fig 5).

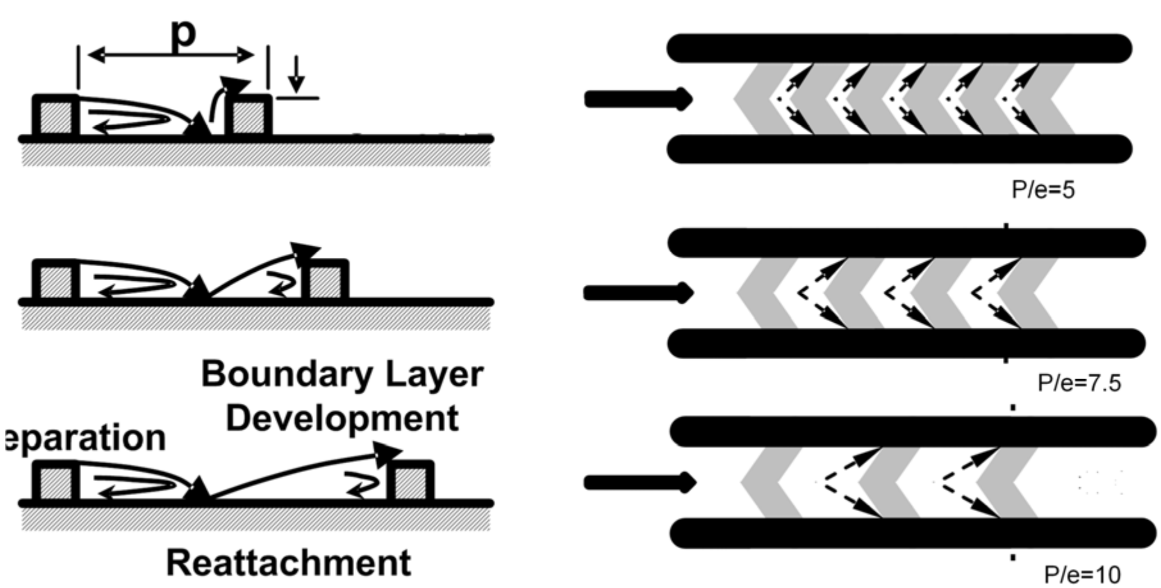

Figure 5 Schematic of flow over V-shape ribs indicating the effect of rib spacing for rib height

The recirculation zone downstream of the rib in each case is same. The boundary layer starts to develop until it is tripped to the next rib. Decreasing the boundary layer development will cause increasing the heat transfer enhancement. . The blockage ratio e/D effects the heat transfer enhancement. If the blockage ratio e/D increases the heat transfer enhancement increase because increasing the blockage ratio enhances the secondary flow. Also increasing the blockage ratio enhances the recirculation zone, the reattachment zone and the developing boundary increase. Fig (6) shows that the heat transfer enhancement decreases if the Reynolds Number increases. This is also consistent with literature [3].

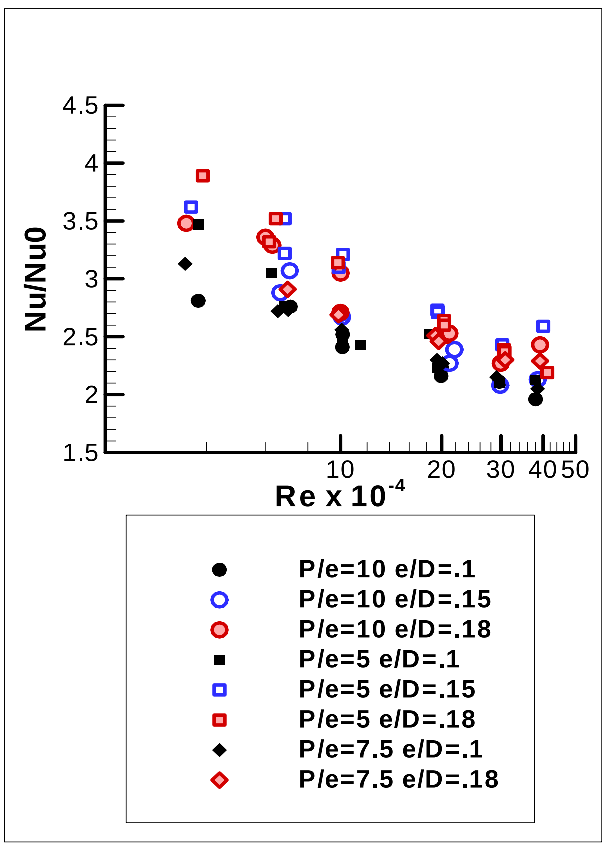

Figure 6 Average normalized Nusselt number with Reynolds number

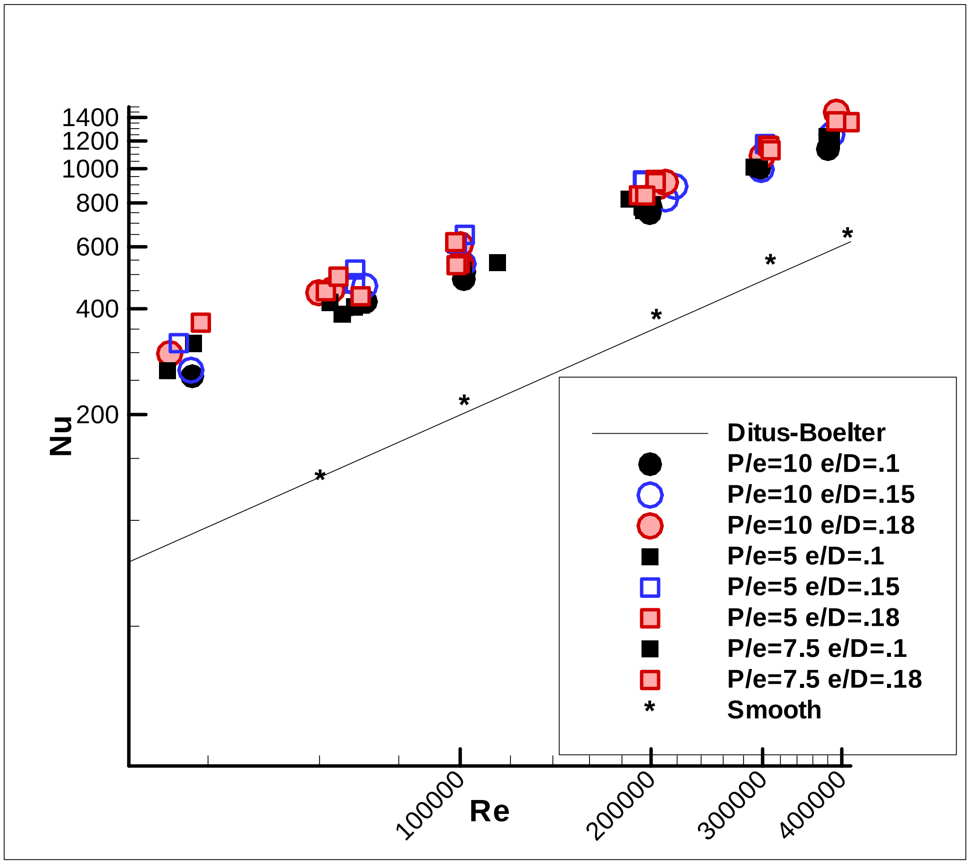

Figure 7 Fully developed ribbed side average Nusselt number obtained in various test cases

The fig (7) shows the relation between Nusselt number and Reynolds number for smooth channel and V-shape ribbed channel in the log- log scale. All seem to be linear. This indicates that the relationship between Nu and Re can be correlated by power law with parameter independent exponent. A correlation is developed by computing a least squares best fit method.

$$Nu = 1.05.(P/e)^{-.1}.Pr^{0.4}.Re^{0.61}.(e/D)^{0.225} \tag{12}$$

30,000 < Re < 400,000, 5 < (P/e) < 10, .1 < e/D <.18

4.2 Friction losses

Decreasing the spacing ratio and increasing the blockage ratio increases the heat transfer enhancement by increasing turbulence and inducing secondary flow. Increasing turbulence and inducing secondary flow causes high friction losses.

In the smooth pipe friction factors are produced by skin-friction. The friction factors are reduced by increasing Reynolds number. In the ribbed channel, the friction factors are produced by form-drag due to the ribs. The flow create separation regions downstream of the rib. Separation region create more pressure drop in the flow.

Fig (8) shows that the friction factor in the ribbed channel is independent of the Reynolds number. The spacing ratio (P/e) effects on the friction factor. If the spacing ratio (P/e) decreases the friction factor increases because the large number of ribs induces greater secondary flow. The blockage ratio e/D effects on the friction factor. If the blockage ratio e/D increase the friction factor increases because increasing the blockage ratio enhance the secondary flow. Also the increasing the blockage ratio enhances the recirculation zone, the reattachment zone and the developing boundary increase. A correlation is developed by computing a least squares best fit method.

$$f = 1.76.(P/e)^{-0.51}.(e/D)^{1.14} \tag{13}$$

30,000 < Re < 400,000, 5 < (P/e) < 10, .1 < e/D <.18

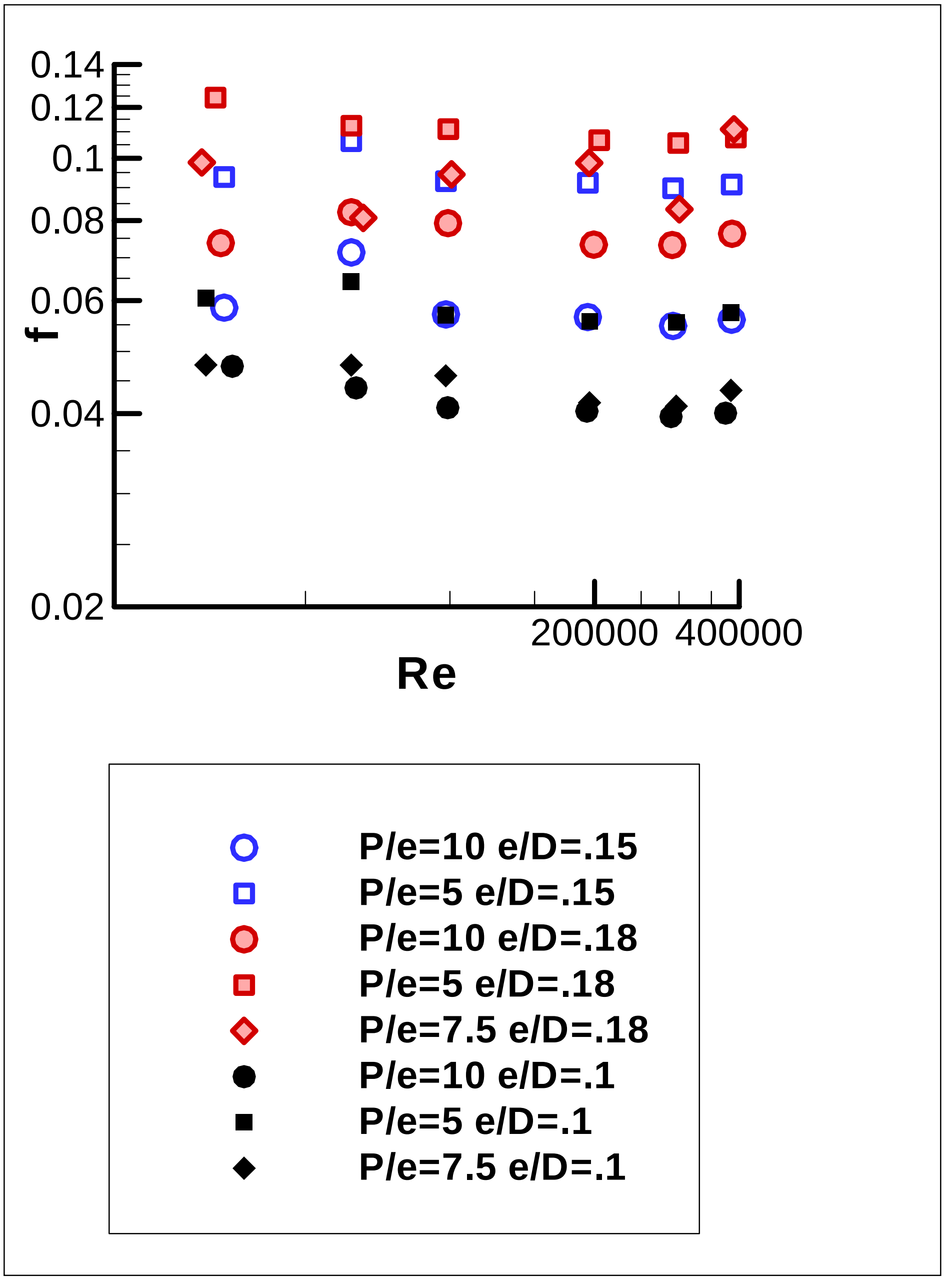

Figure 8 Friction factors for various geometry

4.3 Thermal performance

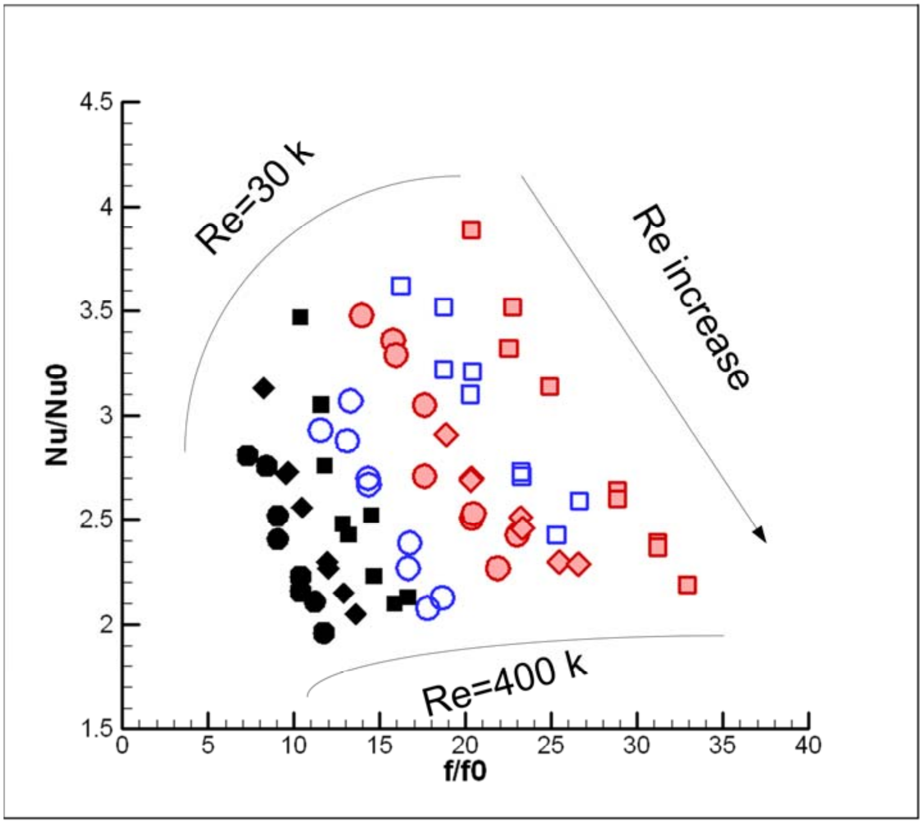

Figure 9 Ribbed side average Nusselt number enhancement ratio plotted against friction factor penalty ratio

Fig (9) shows the relation between the heat transfer enhancement ratio (Nu/Nu_0) and friction factor ratio (f/f_0) for different rib geometries. Fig (9) shows that the heat transfer enhancement ratio decreases and friction factor ratio increases when the Reynolds number increases. The thermal performance (TP) is proportional to the heat transfer enhancement and inversely proportional with cube root of friction factor ratio. Increasing the Reynolds number cause decreasing heat transfer enhancement and increasing the friction factor ratio. Increasing the Reynolds number causes decreasing the thermal performance (see fig 10). Fig 9 shows the e/D=0.1 has the best thermal performance and e/D=0.18 has the worst thermal performance. The P/e=10 has the best thermal performance and P/e=5 has the worst thermal performance.

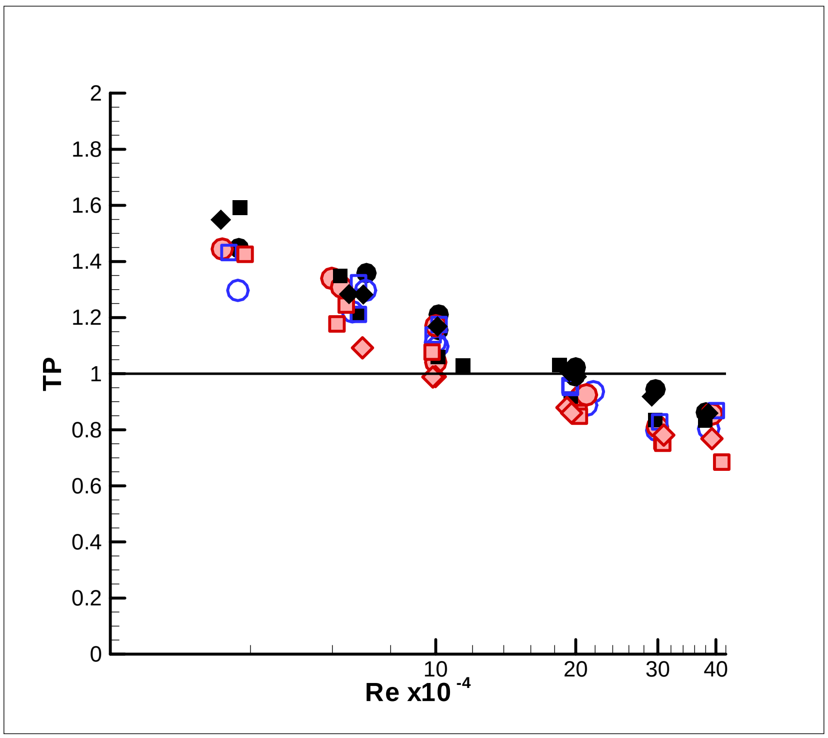

Figure 10 Thermal performance plotted with Reynolds number

5. ERROR ANALYSIS

The experimental uncertainty can be define as

$$e_x = \sqrt{\sum\left(\frac{\partial x}{\partial i}.e_i\right)} \tag{14}$$

where the (e_x) the uncertainty of the (x), (i) measured value, and (e_i) uncertainty of the (i).

5.1 Heat transfer uncertainty

The Heat transfer uncertainty can be calculated by equation (15)

$$e_{Nu} = \sqrt{\left(\frac{\partial Nu}{\partial V}.e_V\right)^2 + \left(\frac{\partial Nu}{\partial \Delta T}.e_{\Delta T}\right)^2 + \left(\frac{\partial Nu}{\partial R}.e_R\right)^2 + \left(\frac{\partial Nu}{\partial X}.e_X\right)^2} \tag{15}$$

where

$$Nu = \frac{V^2}{k.\Delta T.R.X} \tag{16}$$

where (V) is volt, (k) is thermal conductivity, (ΔT) is the temperature deference between the wall temperature and air bulk temperature, (R) the Heater resistance, and (x) is the plate length.

With substation equation (16) to equation (15) the equation (17) is produced.

$$\frac{e_{Nu}}{Nu} = \sqrt{\left(\frac{2.e_V}{V}\right)^2 + \left(\frac{2.e_{\Delta T}}{\Delta T}\right)^2 + \left(\frac{2.e_R}{R}\right)^2 + \left(\frac{2.e_x}{x}\right)^2} \qquad (17)$$

The Hat transfer uncertainty is 2.5 %

5.2 Friction factor uncertainty

The friction factor uncertainty can be calculated by equation (18)

$$e_f = \sqrt{\left(\frac{\partial f}{\partial P}.e_P\right)^2 + \left(\frac{\partial f}{\partial U}.e_U\right)^2} \qquad (18)$$

where

$$\bar{f} = \frac{D}{2\rho u^2}\left|\frac{dP}{dx}\right| \qquad (19)$$

with substation equation (19) to equation (18) the equation (20) is produced.

$$\frac{e_f}{f} = \sqrt{\left(\frac{2.e_p}{P}\right)^2 + \left(\frac{2.e_U}{U}\right)^2} \tag{20}$$

The velocity uncertainty calculated by equation (21)

$$\frac{e_U}{U} = \sqrt{\left(\frac{2.e_p}{P}\right)^2 + \left(\frac{2.e_{\nabla P}}{\nabla P}\right)^2} \tag{21}$$

The friction uncertainty is 9.2 %

6. CONCLUSIONS

The study show effect of the Reynolds number, rib size and rib space on the heat transfer and friction factor. The research show :

- Heat transfer and Friction factor increase due to increase in rib height are due to increase in turbulence in the flow field

- Heat transfer and friction increase when rib-rib spacing is reduced. Heat transfer increases because of both, increasing surface area and increasing turbulence

- Using V-shape ribs instead of Angled ribs edges does not have significant effect on the friction factor. the results in significant improvement in heat transfer

- Thermal performance is below 1 at higher Re friction losses disproportionately higher Nu/Nu0 reduces with increasing Re

- Correlation is presented for Nu and friction factor (for parameter range: $0.1 < e/D < 0.18$; $5 < p/e < 10$, $30,000 < Re < 400,000$)

REFERENCES

1. Je-chin Han , and , Srinath V. Ekkad , Sandip Dutta, 2000, "Gas Turbine Heat Transfer and Cooling Technology," Taylor & Fracis, New York.

2. J. C. Han and J. S. Park, 1988, "Developing heat transfer in rectangular channels with rib turbulators," Int J Heat Mass Transfer, **31**, pp. 183-195.

3. J. C. Han, Y.M Zhang, and C.P.Lee, 1991, "Augmented Heat Transfer in Square channels with parallel, crossed, and V-shaped angled ribs," Journal of Heat Transfer, **113**, pp 591-596.

4. J.C. Han, and Y.M. Zhang, 1992, "High Performance heat transfer ducts with parallel broken and V-shaped broken," Int J Heat Mass Transfer, **35**, pp 513-523.

5. S.C. Lau, R.T. Kukreja, and R.D. Mcmillin, 1991, "Effects of V-shape rib arrays on turbulent heat transfer and friction of fully developed flow in a square channel," Int J Heat Mass Transfer, **34**, pp 1605-1616.

6. J.S. Park, J.C .Han, and S. OU, 1992, "Heat transfer performance comparisons of five different rectangular channels with parallel angled ribs". Int J Heat Mass Transfer, **35**, pp 2891-2903.

7. M.E. Taslim, T. Li , and D.M. Kercher ,1994, "Experimental heat transfer and friction in cannels roughened with angled, V-shape and discrete ribs on two opposite walls," International Gas Turbine and Aeroengine Congress and Exposition ASME, The Hague, Netherlands. June 13-16,1994

8. S.V. Ekkad and J.C Han ,1996, "Detailed heat transfer distributions in two-pass square channels with rib turbulators," Int J Heat Mass Transfer, **40**, pp 2525-2537.

9. M.E. Taslim, and S.D. Spring, 1994, "Effects of Turbulator Profile and Spacing on Heat Transfer and friction in a channel," Journal of Thermophysics and Heat Transfer, **8**, pp 555-561.

10. M.E. Taslim , and C.M. Wadsworth ,1997, "An experimental investigation of rib surface- average Heat Transfer Coefficient in Rib-Roughened Square Passage" Journal of Turbomachinery, **119**, pp 381-389.

11. M.E. Taslim, T.Li, and D.M.Kercher ,1996, "Experimental heat transfer and friction in channels roughed with angled, V-shape, and discrete ribs on two opposite walls," Journal of Turbomachinery, **118**, pp 20-28.

12. M.E. Taslim, and G.J. Korotky, 1998, "Low-aspect-ratio rib heat transfer coefficient measurements in square channel," Journal of Turbomachinery, **120**, pp 831- 838.
13. Rallabandi AP, Yang H, and JC Han, 2008, "Heat Transfer and Pressure Drop Correlations for Square Channels with 45deg Ribs at High Reynolds Numbers," Journal of Heat Transfer, Accepted for publication.

14. Rallabandi AP, ,N. Alkhamis, and JC Han , 2009, "Heat Transfer and Pressure Drop Measurements for a Square Channel With 45deg Round Edged Ribs at High Reynolds Numbers," IGTI, Orlando, Florida, June 8-12.

VITA

Name:	Nawaf Yahya Alkhamis
Address:	Texas A&M University Department of Mechanical Engineering 3123 TAMU College Station, TX 77843
Email Address:	nalkhamis@tamu.edu

Education	B.Sc, Mechanical Engineering, King Abdulaziz University, Jeddah, Saudi Arabia, 2005 M.Sc, Mechanical Engineering, Texas A&M University, College Station, Texas, 2009